1

ZnO Metal-Semiconductor-Metal UV Photodetectors on PPC Plastic with Various Metal Contacts

N.N. Jandow*, H. Abu Hassan, F.K. Yam and K. Ibrahim
Nano-Optoelectronics Research and Technology Laboratory School of Physics Universiti Sains Malaysia, Minden, Penang Malaysia

1. Introduction

The unique and attractive properties of the II-VI compound semiconductors have triggered an enormous incentive among the scientists to explore the possibilities of using them in industrial applications. Zinc Oxide (ZnO) is one of the compound semiconductors of the II–VI family with a direct band gap of 3.37 eV at room temperature, and a large excitation binding energy (60 meV). ZnO is low cost and easy to grow. It is also sensitive to the UV region because of its ultra violet absorbance and has high photoconductivity (Young et al., 2006). These properties make ZnO a promising photonic material for several applications, such as transparent conducting electrodes, surface acoustic wave filters, gas sensors, light emitting diodes, laser diodes and ultraviolet detectors (Kumar et al., 2009; Lim et al., 2006; Janotti et al., 2009; Bang et al.,2003). ZnO is of value and importance due to wide chemistry, piezoelectricity and luminescence at high temperatures. In industry, it can be used in paints, cosmetics, plastics and rubber manufacturing, electronics, and pharmaceuticals [http://www.navbharat.co.in/Clients.htm].

Films of ZnO, indium tin oxide (ITO), and cadmium oxide (CdO) have recently been investigated as transparent conducting oxide (TCO) due to their good electrical and optical properties, their abundance in nature, their optical transmittance (>80%) in the visible region, and they are non-toxic (Angelats, 2006).

ZnO crystallizes in two different crystals structural. The first is the hexagonal wurtzite lattice with lattice constants of a = 3.249 Å and c = 5.207 Å which is mainly used in thin film industry as a transparent conducting oxide (TCO) or as a catalyst in methanol synthesis (Jin, 2003). The second structure, which is well known to geologists, is in the form of rock salt structure which is used in understanding the earth's lower mantle (Hussain, 2008).

ZnO possesses very similar properties to the nitride-based semiconductors such as GaN; yet it has many advantages over GaN (Koch et al., 1985; Paul et al., 2007). For examples: firstly, the growth of high quality single crystal of ZnO is a well understood technology; whereas

* Corresponding Author

for GaN it is difficult. Secondly, the ZnO has large exciton binding energy which means that it has a lower threshold power for lasing. Thirdly, it is one of the few oxides that show quantum confinement in an experimentally accessible range of the size of the particles.

2. Deposition of ZnO on various organic substrates

ZnO thin films traditionally have been deposited on mostly inorganic substrates such as quartz, silicon, glass, sapphire, GaAs, fluorite, mica, GaN, Al_2O_3, diamond, NaCl, and InP (Hickernell, 1976; Ianno et al., 1992; Craciun et al., 1994; Jin et al., 2001; Shan et al., 2004; Sans et al., 2004; Ghosh et al., 2004; Zhang et al., 2004; Tsai et al., 2007; Kiriakidis et al., 2007; Wang et al., 2008) by using different techniques (Mahmood et al., 1995; Auret et al., 2007; Rao et al., 2010; Chakraborty et al., 2008; Hwang et al., 2007; Nunes et al 2010; Sofiani et al., 2006).

The preparation of ZnO thin film on flexible substrates such as plastic has so far received much interest due to its wide variety of applications as in flexible sensors and curved detector arrays. Plastic substrates provide lighter, more resistant to damage, flexible, and durable devices (Nandy et al., 2010); these attributes make them suitable for portable devices such as smart cards, personal digital assistants, digital cameras, cell phones, remote control, and circuits camcorders (Brabec et al., 2001). The substrate materials, that are commonly used for the above applications, include polyethylene terephthalate (PET), polyolefin, polytetrafluoroethylene (Teflon), Polycarbonate (PC), polyarylate (PAR), polyestersulfone (PES), polyimide (PI), poly(ethylene naphthalate) (PEN), thermoplastic polymethyl methacrylate (Perpex, Plexiglas), polyethylene naphthalate, and cellulose triacetate (Ma et al., 2008).

Most of ZnO studies have focused on fabrication issues with little attention given to the structural and optical properties of these films on flexible substrates. Interfacial phenomena in ZnO/polymer heterostructures are expected to be very different from those observed for inorganic substrates, there is a need for more comprehensive investigations to assess the potential of ZnO as a material that can be used in flexible electronic applications. Deposition of ZnO on polymers may open a new opportunities for the creation of novel multifunctional polymer/semiconductor heterostructures.

ZnO thin films deposited on plastics had a number of advantages compared with those on inorganic substrates. From the literature, various types of organic substrates have been explored by researchers to deposited ZnO.

Many researchers (Ott & Chang, 1999; Banerjee et al., 2006; Tsai et al., 2006; Lu et al., 2007) have grown ZnO on PET plastic substrates using different techniques for exemple: Ott and Chang (Ott & Chang, 1999) reported that their samples showed highly transparent ($T > 80\%$) and conductive ($\rho \sim 10^{-3}\ \Omega$ cm) and the best film grown on PET had a resistivity of 1.4×10^{-3} Ωcm. Banerjee *et al* (Banerjee et al., 2006) deposited ZnO thin films with two different thicknesses (~260 and ~470 nm) for 4 and 5 hours using DC sputtering technique. They found that X-Ray diffraction (XRD) pattern for 4 h deposited ZnO films showed a weak intensity as well as broad peak at (002). But the film deposited for 5 h confirmed the formation of crystalline ZnO and three other peaks originated from (100), (002) and (101) reflections of hexagonal ZnO. Their films showed almost 80% to more than 98% visible transmittance and the bandgap (E_g) values were 3.53 eV and 3.31 eV for the films with (~260 and ~470 nm) thicknesses. Room temperature conductivities of the films were found ranging around 0.05 to 0.25 S cm^{-1} and the maximum carrier concentrations around 2.8×10^{16} and 3.1×10^{20} cm^{-3} with a variation in the deposition time of 4 and 5 h respectively.

On the other hand, Tsai *et al* (Tsai et al., 2006) reported that their ZnO/PET films showed a strong (002) peak from XRD measurements and the scanning electron microscopy (SEM) morphology of the films showed that no crack or bend appeared on the films. The average transmittance in the visible spectrum was above 80% for both substrates and the value of E_g was found equal to 3.3 eV. The lowest resistivity obtained was 4.0×10^{-4} Ω cm. Lu *et al* (Lu et al., 2007) found that XRD results of their deposited thin films showed a strong peak at (002) orientation and the root mean square (rms) were in the range 2.63~11.1 nm determined by atomic force microscopy (AFM). The average transmittance of the film was obtained over 80% in the visible spectrum. The lowest resistivity obtained was 4.0×10^{-3} Ωcm.

Whereas, Liu *et al* (Liu et al., 2007) deposited ZnO thin film at the first time on Teflon substrate by the rf magnetron sputtering. They reported that the XRD pattern of the film showed a strong peak at $2\theta = 34.283°$ which corresponding to the (002) peak with full-width at half-maximum (FWHM) of 0.724° and the film also showed other peaks such as (100), (101), (102), (103) and the crystallite size was equal to 10 nm. The SEM image of ZnO thin film showed that the ZnO film structure consists of some columnar structured grains.

On the other hand, Kim et al (Kim et al., 2009) deposited ZnO films on PC and PES substrates by using rf sputtering system. They studied the effect of sputtering power ranged from 100 to 200 W on the characteristics of the films. XRD patterns of their deposited films showed strong 2θ peaks at 34.4° and they found that the intensities of the ZnO (002) peak and the grain size increased with increasing the sputtering power. The transmittance of the films on both substrates was 80-90%.

Also Liu et al (Liu et al., 2009) prepared Transparent conducting aluminum-doped zinc oxide (ZnO:Al) films on PC substrates by pulsed laser deposition technique at low substrate temperature (room-100 °C. they reported that their experiments were performed at various oxygen pressures (3 pa, 5 pa, and 7 Pa). they studied the influence of the process parameters on the deposited (ZnO:Al) films. X-ray diffraction for their prepared films showed polycrystalline ZnO:Al films having a preferred orientation with the c-axis perpendicular to the substrate were deposited with a strong single violet emission centering about 377–379 nm without any accompanying deep level emission. The average transmittances exceed 85% in the visible spectrum.

Other organic substrates such as polyimide (Paul et al., 2007 and Craciun et al., 1994), polyarylate (Ianno et al., 1992), PEN (Koch et al., 1985) have also been tried by other researchers to deposit ZnO thin film. These ZnO thin films have been used to fabricate thin film transistor (TFT). The fabricated ZnO TFT on various organic substrates showed very encouraging results.

In summary, ZnO thin film deposited on organic substrates by different techniques are in the polycrystalline form with (002) orientation as the dominant peak. The thin films grown on these substrates usually demonstrated good optical transmittance characteristic, i.e. above 80% and the bandgap could be varied from 3.31-3.53 eV. In addition, the carrier concentration is dependent on the growth condition. Overall the ZnO thin films quality on organic substrates is comparable to those in organic substrates.

3. An overview of photodetectors

Photodetectors are basically semiconductor devices that convert the incident optical signal into an electrical signal which is usually revealed as photocurrent. The photodetectors can detect the optical signals over a range of the electromagnetic spectrum that is usually predominantly defined based on the material properties. A detector is selected based on the requirements of a particular application. The general requirements include wavelength of light to be detected, sensitivity level needed, and the response speed. In general, photodetectors respond uniformly within a specific range of the electromagnetic spectrum. Consequently, the wavelength of light detected determines the selection of the photodetector material and the target application and defines the structure (Sze, 2002). This will be explained further in the following sections.

When the incident photons with energy higher than the bandgap energy of a semiconductor; some of them will be absorbed within the semiconductor layer. Such a successful absorption process results in the generation of a free electron-hole pair. The energy gained by the electron which is called the work function must be sufficient to make the electron cross the barrier height between the metal contact and the semiconductor with kinetic energy (E_e). The kinetic energy can be given as (Sze, 2002).

$$E_e = \frac{hc}{\lambda} - \phi_m \tag{1}$$

where c is the light velocity, ϕ_m is the metal work function and λ is the incident wavelength.

Since the photoelectric effect is based on the photon energy hv, the wavelength of interest is related to energy transition ΔE in the device operation, with the following relationship:

$$\lambda = \frac{hc}{\Delta E} = \frac{1.24}{\Delta E(eV)} \qquad (\mu\text{m}) \tag{2}$$

where ΔE is the transition of energy levels.

Because the photon energy $hv > \Delta E$ can also cause excitation, Eq. 2 is often the minimum wavelength limit for detection. The transition energy ΔE, in most cases, is the energy gap of the semiconductor. It depends on the type of photodetector, and it can be the barrier height as in a metal-semiconductor (MS) photodiode. Alternatively, the transition energy can be between an impurity level and the band edge as in an extrinsic photoconductor. The type of photodetector and the semiconductor material are normally chosen and optimized for the wavelength of interest. The absorption of light in a semiconductor is indicated by the absorption coefficient. The transition energy does not only determine whether light can be absorbed for photoexcitation, but it also indicates where light is absorbed. A high value of absorption coefficient indicates light is absorbed near the surface where light enters. Whilst, a low value means the absorption is low that light can penetrate deeper into the semiconductor (Sze & Kwok 2006).

3.1 Semiconductors for UV photodetection

UV detection has usually been applied to narrow bandgap semiconductor photodiodes, thermal detectors, photomultiplier tubes (PMT), or charge-coupled devices (CCD) because they exhibit high gain and low noise and they can be rather visible-blind. However, PMT is a fragile and bulky device which requires high power supplies. On the other hand, CCD detectors are slow and their response does not depend on the wavelength. Semiconductor photodetectors require only a mild bias, and can be benefited for their small size and light weight, and being insensitive to magnetic fields. Their low cost, good linearity and sensibility, and capability for high-speed operation make them excellent devices for UV detection (Monroy et al., 2003).

The main disadvantage of these narrow-bandgap semiconductor detectors is device aging due to the exposure to radiation that has much higher energy than the semiconductor bandgap. Moreover, passivation layers, typically SiO_2, reduce the quantum efficiency in the deep-UV range, and are also degraded by UV illumination (Caria et al., 2001)[43]. Another disadvantage of these devices is their sensitivity to low energy radiation, eventually, filters are required to block out visible and infrared photons, resulting in a significant loss of the effective area of the device. Finally, for high-sensitivity applications, the detector active area must be cooled to reduce the dark current. The cooled detector behaves as a cold trap for contaminants which leads to a lower detectivity (Monroy et al., 2003). Such problems make the wide-bandgap semiconductors, such as gallium nitride and ZnO, attractive alternatives. Therefore, ZnO has been used in optoelectronic, high power and high frequency devices.

3.1.1 Wide-bandgap semiconductors for UV photodetection

Detection of ultraviolet (UV) radiation is increasingly becoming important in a number of areas, such as flame detection, water purification, furnace control, UV astronomy, UV radiation dosimetry (Lakhotia et al., 2010).

Even though the responsivity of Si-based optical photodetectors in the UV region is low, they are still being used for light detection (Lakhotia et al., 2010). This has promoted some researchers to use wide direct band gap materials to fabricate optoelectronic devices that are sensitive in the UV region. Hence, GaN-based UV photodetectors have already become commercially available (Hiramatsu et al., 2007). ZnSe-based UV photodetectors, which is another wide direct band gap material, have also been manufactured (Hanzaz et al., 2007). Fabrication and characterization of low-intensity ultraviolet metal-semiconductor-metal (MSM) photodetectors based on AlGaN have also been reported (Gökkavas et al., 2007). ZnO is another semiconductor of wide direct bandgap that is also sensitive in the UV region and is of low cost and easy to manufacture. Therefore, ZnO will be focused in this chapter.

The importance of semiconductor UV PD has expanded the semiconductor industry and emphasized the development of low-light-level imaging systems for military and civilian surveillance applications. These detectors should:

1. not be sensitive to light at visible wavelengths (commonly referred to as being solar blind),
2. have a large response at the wavelength to be detected and have high quantum efficiency,
3. have a small value for the additional noise introduced by the detector.

There are many different types of semiconductor ultraviolet photodetectors such as: photoconductive or photoconductors detectors, p-n junctions photodiode, and MSM (metal-semiconductor-metal) photodetector (Liu et al., 2010). In the field of optical devices, several trends are pushing research to use new materials. For example, the UV PD is successfully fabricated based on wide bandgap semiconductors (E_g > 3.0 eV). Photon detectors may be further subdivided according to their physical effects that make the detector responsive.

3.1.2 Metal-Semiconductor-Metal (MSM) photodiodes

Metal-semiconductor-metal (MSM) is a type of PD used for UV detection. MSM PDs consist of two interdigitated Schottky contacts which are called fingers deposited on top of an active layer as shown in Figure 1. These devices have a fast response and simple structure compared to other photodetectors of the same active area because of the interdigitated structure which reduces carrier transit time through close spacing of the electrodes, while maintaining a large active area.

The MSM PD operates when the incident light is directed on the semiconductor material between the fingers, electrons will be generated in the conduction band, and thus creating holes in the valance band of the undoped region of the semiconductor. This results in creating a photocurrent by means of one of two processes with the operative process determined by the magnitude of the incident photon energy (*hv)* relative to the energy bandgap (E_g) of the semiconductor and the metal work function (ϕ_{Bn}). If E_g is greater than *hv* and *hv* is greater than ϕ_{Bn}, then photoelectric emission of electrons from the metal to the semiconductor occurs. Alternatively, for the second process, if *hv* is greater than E_g, then photoconductive electron-hole pairs are produced in the semiconductor. The generated electrons and holes are separated by an electric field intrinsically formed between the fingers.

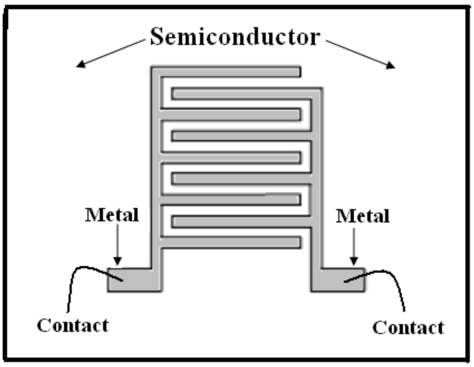

Fig. 1. Top view of an MSM PD planar interdigitated structure

4. ZnO as a UV detector

As mentioned before, ZnO is one of the most prominent semiconductors in the metal-oxide family because of its excellent properties which attract many researcher groups to use this material in UV detection applications. Below, a briefly discussion of ZnO as a UV detector will present and some earlier studies about the fabrication of ZnO as UV detector will also be provided.

ZnO was one of the first semiconductors to be prepared in a rather pure form after silicon and germanium. It was extensively characterized as early as in the 1950`s and 1960`s due to its promising properties (Plaza et al., 2008). Wide band gap semiconductors have so far gained much attention for the last decade because they can be used in optoelectronic devices in the short wavelength and also in the UV region of the electromagnetic spectrum. These

Wide band gap semiconductor	**Crystal structure**	**Lattice parameter (Å)**		**E_g (eV) at RT**	**Melting temp. (K)**	**Excitation binding energy (meV)**
		a	*c*			
ZnO	Wurtzite	3.25	5.206	3.37	2248	60
GaN	Wurtzite	3.189	5.185	3.4	1973	21
ZnSe	Zinc-blende	5.667	-	2.7	1790	20
ZnS	Wurtzite	3.824	6.261	3.7	2103	36
4H-SiC	Wurtzite	3.073	10.053	3.26	2070	35

Table 1. Comparison of different semiconductors (Tüzemen & Gür, 2007; Nause & Nemeth, 2005) Note: Where RT is room temperature, meV is millielectron volt.

Sab.	**D.M.**	**PD T**	**R. C.**	**O. C.**	**B.V. (V)**	**I_d (A)**	**I_{ph} (A)**	**λ (nm)**	**R (A/W)**	**Ref**
Sapp.	MOCVD	MSM UV	-	Al	5	1×10^{-6}	-	-	1.5	(Liang et al., 2001)
GaAs	rf	p-n HJ	-	-	~3.0	-	$\sim 2 \times 10^{-3}$	325	-	(Moon et al., 2005)
p-Si (100)	rf		Au-Al	In	30	-	-	310	0.5	(Jeong et al., 2004)
Sapp.	Sol–gel	MSM UV	Au	-	-	-	-	350	0	(Basak et al., 2003)
Sapp.	MOCVD	MSM	Al	Al	5	450×10^{-6}	-	-	400	(Liu et al., 2000)
Quar.	rf	MSM UV	Au	Au	3	250×10^{-6}	-	360	30	(Liu et al., 2007)
Sapp.	PA MBE	UV		Al-Ti	20		-	374	1.7	(Mandalapu et al., 2007)
SiO_2	rf	MSM UV	Au	Au	3	1×10^{-3}	-	-	0.3	(Jiang et al., 2008)
Sapp.	rf	MSM UV	Ir	Ir	-	-	-	370	0.2	(Young[a] et al 2007)
Sapp.	rf	MSM UV	Pd	Pd	1	-	-	370	0.1	(Young[b] et al., 2007)
Sapp.	MBE	MSM UV	Ru	Ru	-	8×10^{-8}	1.8×10^{-5}	-	-	(Lin et al., 2005)

Sab = Substrate; D.M. = Deposition method; PD T. = PD type; B.V. = Bias voltage R C. = Rectifying contacts; O. C. = Ohmic contact; I_d = Dark current; I_{ph}= Photocurrent; λ = Wavelength; Sapp. = Sapphire; Quar. = Quartz; ED = Electrochemical deposition; PAMBE = Plasma-assisted molecular-beam epitaxy; p-nHJ = p-n homojunction

Table 2. Summarizes the characteristics of ZnO UV PDS reported by other researchers fabricated by different methods

semiconductors which include ZnO, GaN, ZnSe, ZnS, and 4H-SiC have shown similar properties with their crystal structures and band gaps (Tüzemen & Gür, 2007).

Table 1 below shows a summary of some of the important properties of these wide band gap semiconductors. Initially, ZnSe and GaN based technologies made significant progress in the blue and UV light emitting diode and injection laser. No doubt, GaN is considered to be the best candidate for the fabrication of optoelectronic devices. However, ZnO has great advantages for light emitting diodes (LEDs) and laser diodes (LDs) over the currently used semiconductors. Recently, it has been suggested that ZnO is promising for various technological applications, especially for optoelectronic short wavelength light emitting devices due to its wide and direct band (Nause & Nemeth, 2005).

From the literature ZnO UV PDs have been widely investigated by many researchers on different substrates through different methods. Table 2 compiles and summarizes the structural of ZnO UV PDS reported by other researchers.

5. Schottky barrier height calculation of MSM PD

A MSM PD is a unipolar device with two back-to-back Schottky junctions formed on the same semiconductor surface. Under the application of bias voltage, one of the diodes becomes reverse biased, forming a depletion region that tends to sweep out photocarriers. The other diode becomes forward biased, allowing the collected photocurrent to flow out just as an ohmic contact. Under sufficiently high bias voltage, the depletion region extends and touches the small space-charge region under the forward biased electrode.

Figure 2 shows the energy-band diagram of the MSM PD in the biased state. The vertical displacement of the electrode metals indicates the bias voltage applied to the device resulting in the forward biased condition of the left-hand metal-semiconductor interface and the reverse bias of the right-hand interface. Upon biasing, the semiconductor between the electrodes becomes fully depleted of free carriers. The reversed biased interface prevents the current from flowing through the device when there is no optical signal. The depleted regions between the electrodes are the photodetector active regions. As mentioned before, a photon with energy greater than the band gap of the semiconductor will be absorbed by an electron; this electron will get excited to the conduction band as shown by the process labeled as (1) in Figure 2. The photogenerated electron and hole are swept by the high applied fields to the positive and negative electrodes resulting in an electronic output signal (Haas, 1997).

One can assume that other current transport processes also contribute to the movement of electrons within the depletion region and across the barrier in Schottky contacts to determine the barrier height. The equations usually used to determine the barrier height in a Schottky diode. Assuming pure thermionic emission and V>3KT, the general I–V equations usually used to determine the barrier height in a Schottky diode are represented by (Daraee et al., 2008)

$$I = I_0 \exp[qV / (nKT)] \tag{3}$$

$$I_0 = A^* AT^2 \exp[-q\phi_B / (KT)] \tag{4}$$

where I_0 is the saturation current, n is the ideal factor, K is the Boltzmann's constant, T is the absolute temperature, ϕ_B is the barrier height, A is the area of the Schottky and A^* is the effective Richardson coefficient. Eq. 4 indicates the dependence of the barrier height on the saturation current (I_o). The theoretical value of A^* can be calculated using Eq. (5) below.

$$A^* = 4\pi m^* q K^2 / h^3 \tag{5}$$

where h is Planck's constant and $m^* \sim 0.27 m_o$ is the effective electron mass for n-type ZnO so that $A^* \sim 32\ A/cm^2K^2$ (Liang et al 2001).

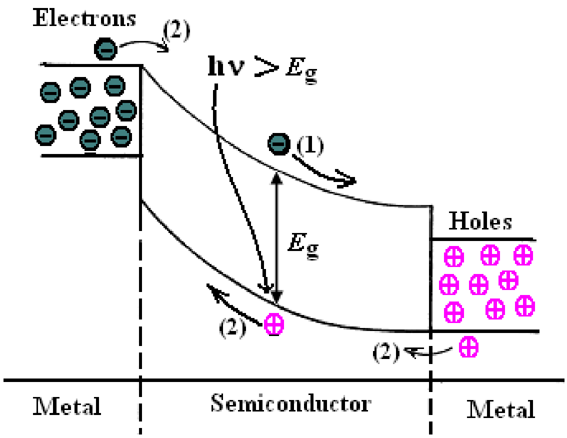

Fig. 2. Energy-band diagram of MSM detector indicating; (1) the photogeneration of signal charges and (2) the thermally-generated carriers overcoming barrier heights adding to device dark current

MSM-PD performance is critically dependent on the quality of the Schottky contacts. Therefore, it is necessary to measure the Schottky barrier height of the actual contact which is a constituent part of the MSM PD under investigation. As mentioned before, a MSM-PD essentially consists of two Schottky contacts connected back-to-back. When a bias is applied within the MSM; this will put one Schottky barrier in forward direction (anode) and the other is reverse direction (cathode).

Following the analyses of Sze (Sze et al., 1971), one can get the approximate dark current formula of the MSM PD. The current transported over the Schottky barrier height as a function of the applied voltage by considering both electron and hole current components here has the general expression as (Sze & Kwok 2006)

$$I_{da} = A_1 A_n^* T^2 \exp\left(\frac{-q\phi_{Bn}}{KT}\right) + A_2 A_p^* T^2 \exp\left(\frac{-q\phi_{Bp}}{KT}\right) \tag{6}$$

where A_1 and A_2 are the anode and cathode contact areas respectively; A_n^* and A_p^* are the effective Richardson constants; and ϕ_{Bn} and ϕ_{Bp} are the barrier heights for electrons and holes respectively. For a semiconductor with wide bandwidth, the Schottky barrier of the hole is high, and the hole is a minor carrier. Hence the hole current can be neglected, assuming that the dark current can mostly consist of the electron current (Jun at al., 2003). The dark current of the MSM PD is approximately as shown below (Yam & Hassan, 2008)

$$I = I_0 \exp[qV / (nKT)][1 - \exp(-qV / KT)] \tag{7}$$

Thus, Equation (6) can be re-written follows:

$$\frac{I \exp[qV / (KT)]}{\exp[qV / (kT)] - 1} = I_0 \exp[qV / (nKT)] \tag{8}$$

Based on Eq. (8), the plot of $\ln\left\{I \exp\left(qV / \{KT\}\right) / \left[\exp\left(qV / \{KT\}\right) - 1\right]\right\}$ vs. V results in a straight line; I_0 is derived from the interception with y-axis as shown in Figure 3. Schottky barrier height ϕ_B at the MS interface can be obtained by substituting I_0 value in Eq. (4).

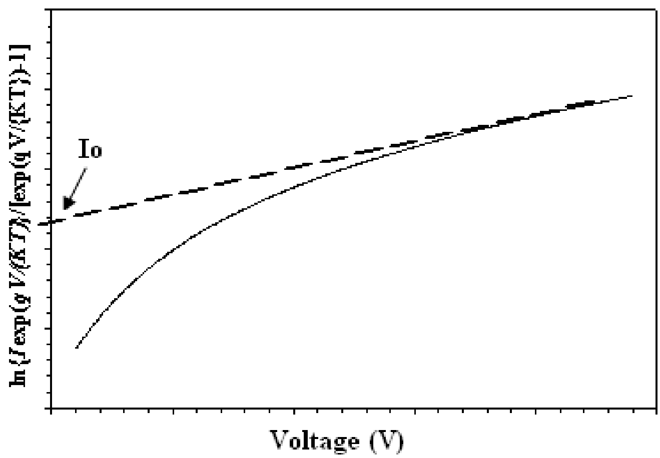

Fig. 3. $\ln\left\{I \exp\left(qV / \{KT\}\right) / \left[\exp\left(qV / \{KT\}\right) - 1\right]\right\}$ vs.V of a MSM PD

6. Photodetectors characteristics

There are many characteristics that describe the performance of a PD. These performance characteristics indicate how a detector responds. The response of the detector should be great at the wavelength to be detected. Whilst, the additional noise created by the detector should be small. The response speed should be high so that the variations in the input optical signal can also be detected. The performance characteristics of the photodetectors are summarized in the following subsections.

6.1 Responsivity (R)

Responsivity is defined as the ratio of the photocurrent output (in amperes) to the incident optical power (in watts). It is expressed as the absolute responsivity in amps per watt (A/W). Therefore, responsivity is to measure the effectiveness of the detector for converting the electromagnetic radiation to the electrical current. Responsivity depends on wavelength, bias voltage, and temperature. Reflection and absorption characteristics of the detector's material change with wavelength and hence the responsivity also changes with wavelength (Sze & Kwok 2006).

The responsivity in terms of the photo current can be written as:

$$R = \frac{I_{ph}}{P_{inc}} = \frac{\eta q}{h\nu} \tag{9}$$

where I_{ph} is the photo current (A), P_{inc} is the incident optical power (W), η is the external quantum efficiency of the PD.

The responsivity in terms of wavelength can also be written as:

$$R = \frac{\eta \lambda q}{hc} = \frac{\eta \lambda (\mu m)}{1.24} \text{ (A/W)} \tag{10}$$

where λ is the incident wavelength.

Responsivity is an important parameter that is usually specified by the manufacturer. Through responsivity, the manufacturer can determine how much detector's output is required for a specific application.

6.2 Quantum efficiency

Quantum efficiency of a photodetector (QE) (η %) is defined as the ratio of the electron generation rate to the photon incidence rate. QE is related to the photodetector responsivity by the following equation (Sze & Kwok 2006):

$$\eta = \frac{I_{ph}/q}{P_{inc}/h\nu} = \frac{I_{ph}}{q} \cdot \frac{h\nu}{P_{inc}} \tag{11}$$

7. Characteristics of ZnO thin films deposited on PPC plastic

From the literature, the deposition of ZnO thin film on organic substrate such as PPC has not been reported by other groups. Therefore, PPC shows great potential as a substrate for ZnO thin film. The PPC has been chosen for its excellent properties such as low cost, high dielectric strength and high surface resistivity; and it is considered as one of the important polymers for biomedical and engineering application (Zhang et al., 2007). It also exhibits high transparency and superior mechanical strength (Song et al., 2009). These attractive

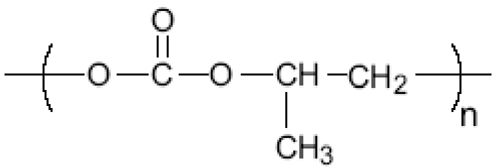

Fig. 4. The chemical structure of Poly (propylene carbonate) (PPC)

properties make the PPC a good substrate for a variety of microelectronic applications. Figure 4 shows the chemical structure of PPC plastic (Lu et al., 2005). This section briefly presents the structural, optical and electrical properties of ZnO deposited on PPC substrate.

7.1 The structural properties

ZnO thin film had been deposited on PPC plastic substrate with thickness of the 1μm. In order to study the structure of the film, XRD diffraction pattern of the deposited ZnO thin film on PPC plastic substrate was measured as shown in Figure 5. The XRD pattern shows that the film is ZnO as compared to the International Center for Diffraction Data (ICDD) library, and it is oriented in c-axis, which is the preferred orientation axis for such a material.

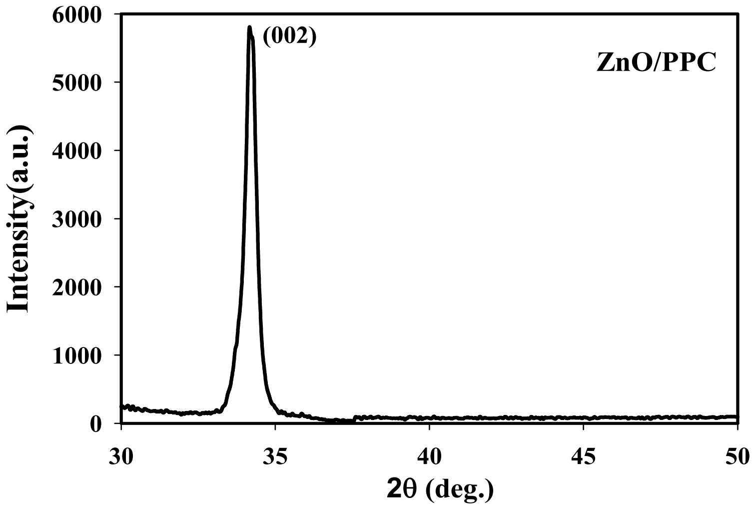

Fig. 5. XRD diffraction for ZnO thin film on PPC plastic substrate

The film shows a strong peak at 2θ = 34.27° which is correlated to the characteristic peak of the hexagonal ZnO (002) with full width at half maximum (FWHM) of 0.31°. The small FWHM of the ZnO (002) XRD peak again indicates good crystal quality of the sample (Jandow et al., 2010a).

The grain size also calculated from the FWHM of the XRD spectrum based on Scherrer formula as in Eq. 12 (Tan et al., 2005) was found to be about 26.8 nm.

$$D = \frac{K\lambda}{B\cos\theta} \tag{12}$$

where B is the full width at half maximum[(FWHM) in radians] intensity of XRD, λ is the X-ray wavelength (Cu $K\alpha$ =0.154 nm), θ is the Bragg diffraction angle, and K is a correction factor which is taken as 0.9 (Tan et al., 2005). Thus we can conclude that the film deposited on PPC plastic is nanostructured crystal. This finding is in agreement with the result reported by Myoung *et al* (Myoung et al., 2002).

The surface morphology of the film was studied using SEM as shown in Figure 6. The figure shows that the ZnO has smooth surface morphology and relatively smaller particles, which are well connected to each other; it strongly adheres to the substrate and has tightly bounded particles. Inset in Figure 6 shows the SEM image reported by Ergin *et al* (Ergin et al., 2009). A close visual inspection reveals that the prepared sample in this work has similar surface morphology as reported by Ergin. These good surface properties have strong effect on the optical properties such as transmittance and absorbance of the UV light when this material is used as UV detector (Jandow et al., 2010b).

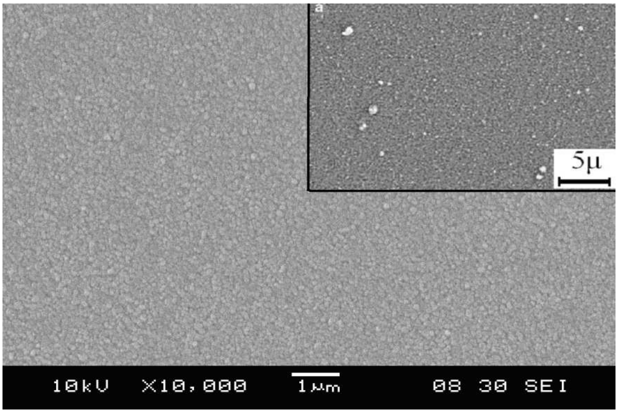

Fig. 6. SEM image of ZnO film on PPC substrate

The elemental analysis of the sample was investigated by EDX as shown in Figure 7.The EDX result shows that Zn, O and C elements were present in the sample. Zn and O elements came from ZnO film, on the other hand, C element was not anticipated in the film; obviously, the presence of C was due to the PPC substrate. Similarly, Ergin *et al* (Ergin et al., 2009) who studied the properties of ZnO deposited on glass substrate pointed out that Si and Ca elements were not expected to be in ZnO film and these two elements could have come from the glass substrates. The inset in Figure 7 shows the EDX image reported by them.

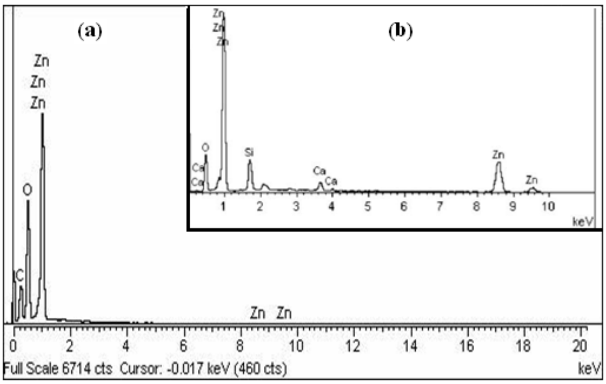

Fig. 7. (a) EDX image of ZnO film on PPC substrate. (b) Inset shows the EDX image from Ref. (Ergin et al., 2009)

The film surface was examined by AFM as shown in Figure 8. A typical AFM image shows that ZnO thin film consists of some columnar structure grains with root mean square (rms) equal to 10 nm; this nanostructure of the film surface may be useful in the absorption of the UV light when this material is used as a UV detector (Jandow et al 2010c).

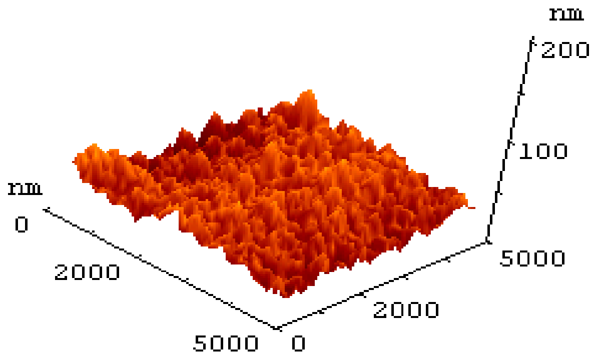

Fig. 8. AFM image of ZnO on PPC substrate (rms =10 nm)

7.2 The optical properties

The PL of the prepared ZnO thin film on PPC plastic was measured at room temperature. The result is given in Figure 9. Two luminescence peaks can be found in the figure. The first luminescence peak is the UV emission of ZnO thin films at 379.5 nm and as mentioned before it corresponds to the near band edge emission (NBE) due to the electronic transition from the near conduction band to the valence band as reported by Young *et al* and Gao and Li (Young et al., 2006; Gao &Li 2004).

The other luminescence peak is the blue-green emission ranged from 452.0 to 510.0 nm as shown in the inset in Figure 9, which is due to the defect related to deep level emission (Tneh et al., 2010). This result is in agreement with Wei *et al*. and Wu *et al* (Wei et al., 2007; Wu et al., 2007), which is attributed to the transition of electron from defect level of Zn interstitial atoms to top level of the valence band. In addition, the high UV to the visible emission ratio indicates a good crystal quality of the film which means a low density of surface defects (Jandow et al., 2010b).

The transmission and absorption spectra of ZnO film are shown in Figure 10. It can be seen that the transmission values of the film are low at short wavelengths (≤ 380nm) and high at long wavelengths. Therefore, the film behaved as an opaque material because of its high absorbing properties at short wavelengths as shown in the same figure and as a transparent material at long wavelengths.

This situation is related to the energy of the incident light; when energies of photons are smaller than the bandgap of ZnO film, they are insufficient to excite electrons from the valence band to the conduction band. However, ZnO has oxygen vacancies and interstitial Zn atoms, which act as donor impurities (Jandow et al., 2010d).

These impurities may be ionized by these low energies, so the film has low absorbance and high transmittance values at long wavelengths. The transmittance values increased higher than 80% in the visible region remarkably as the wavelength increased and this range refers to the fundamental absorption region (Shan et al., 2005). This indicates that the film could be used as transparent windows for UV light or as electrodes in a metal-semiconductor-metal MSM PDs (Jandow et al., 2010e).

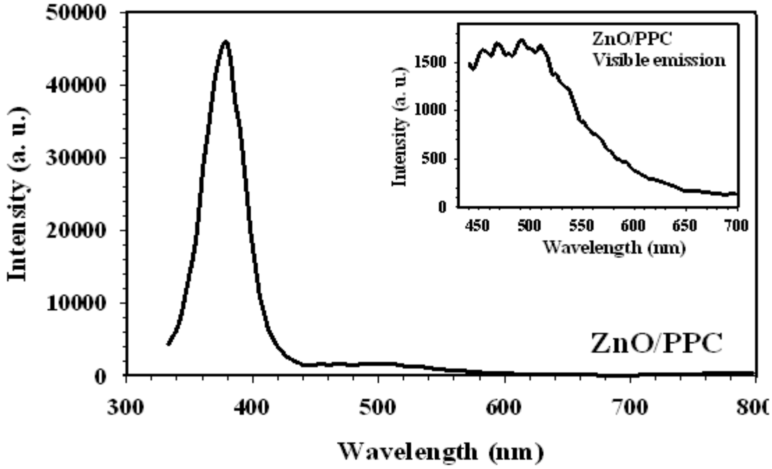

Fig. 9. Room temperature PL spectrum of DC- sputtered ZnO on PPC substrate. Inset shows the expansion of visible emission of ZnO thin film

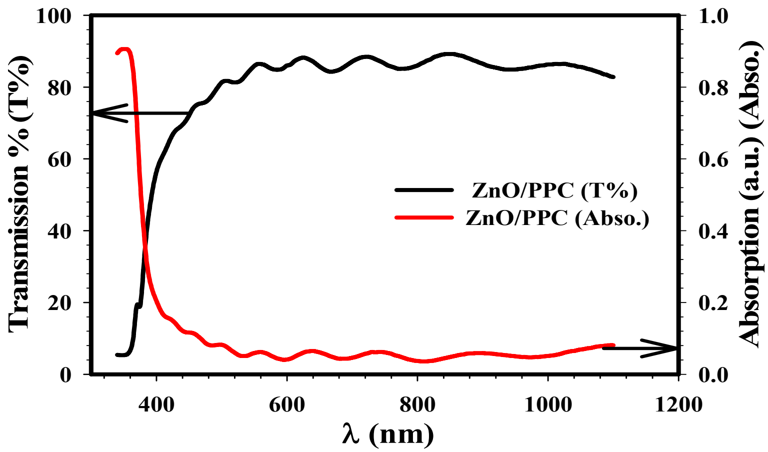

Fig. 10. Transmission and absorption spectra of ZnO thin film on PPC substrate

As mentioned earlier; ZnO is a wurtzite structure semiconductor with a direct band gap of 3.37 eV at room temperature. The absorption coefficient of the direct band gap material is given by the Eq. (Shan et al., 2005)

$$\alpha(h\nu) \propto (h\nu - E_g)^{1/2} \tag{13}$$

The dependence of $(\alpha h\nu)^2$ against the photon energy ($h\nu$) is plotted as in Figure 11. By extrapolating the linear part of the plot to $(\alpha h\nu)^2 = 0$ the value of the energy gap was found to be about 3.33 eV.

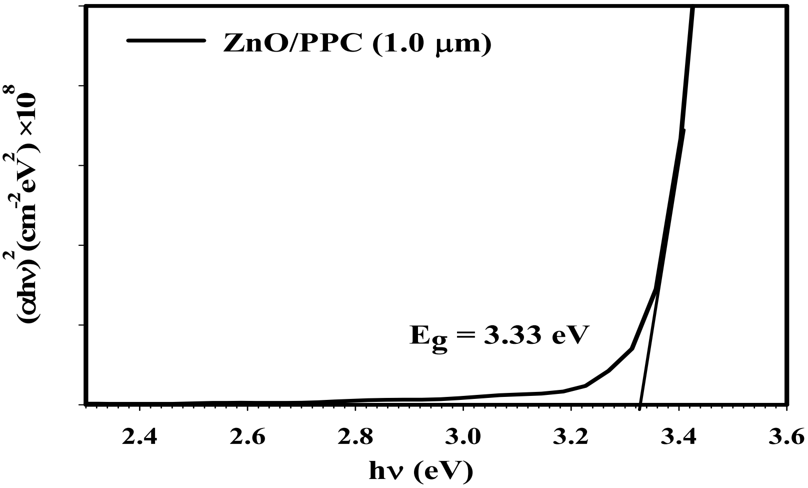

Fig. 11. The bandgap derivation for ZnO thin film on PPC substrate from the dependences of $(ah\nu)^2$ on $h\nu$

Similar results were reported by Banerjee *et al* (Banerjee et al., 2006) who deposited ZnO thin film on PET plastic substrate and also by many other authors who prepared their ZnO thin films on glass and silicon (Gümüş et al., 2006; Khoury et al., 2010; Kang et al., 2007; Lai et al., 2008).

7.3 The electrical properties

The Hall measurements show that the film is n-type with resistivity, ρ, of about 1.39×10^{-1} Ω-cm and mobility, μ, of 26 cm²/V-s. The carrier concentration, n, was measured and it was found to be 1.72×10^{18} cm^{-3}.

Substrate	ZnO Electrical properties			Ref.
	Resistivity, ρ (Ω-cm)	Mobility, μ(cm²/V-s)	Carrier concentration, n (cm^{-3})	
PPC	1.39×10^{-1}	26.00	1.72×10^{18}	In this work
PET	1.00×10^{-3}	N.A.	N.A.	(Ott et al., 1999)
PET	N.A.	19.82	2.80×10^{16}	(Banerjee et al., 2006)
PET	4.0×10^{-3}	N.A.	N.A.	(Tsai et al., 2006)

Table 3. Some of the reported ZnO electrical properties on organic substrates

From the literature, the electrical properties of ZnO thin film deposited on organic substrates have rarely been reported. Table 3 summarizes some of the reported electrical properties. From the table, it was found that the resistivity value for our sample is about two orders of magnitudes higher than typical reported values (Ott et al., 1999; Tsai et al., 2006) and the mobility, μ, is 1.3 times higher than the results in (Banerjee et al., 2006). On the other hand, the carrier concentration, n, of our sample is about two orders of magnitudes higher as compared to the reported value in Ref (Banerjee et al., 2006).

8. The characteristics of ZnO UV PDs prepared on PPC

ZnO UV PDs with different metal contacts i.e. Pd, Ni and Pt have been fabricated on PPC plastic substrates. Figure 12 shows the fabricated ZnO UV PD with Pd contacts. The UV detector fabricated on PPC is very flexible and low cost.

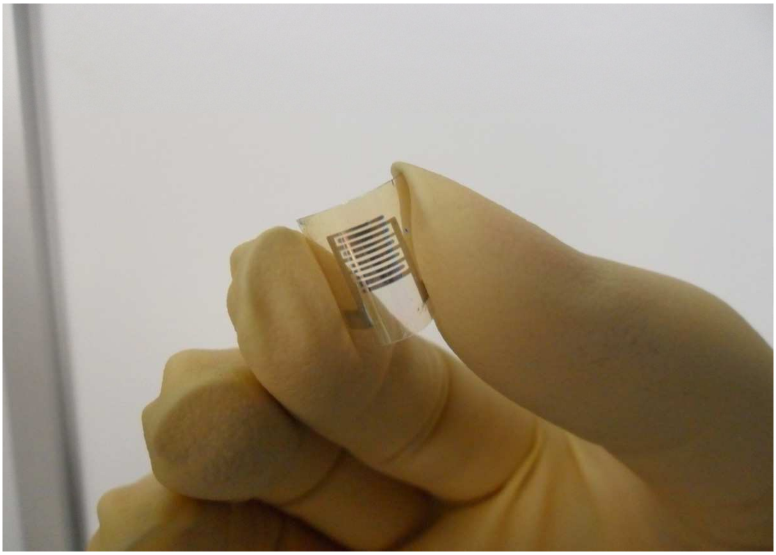

Fig. 12. The ZnO UV PD fabricated on PPC plastic with Pd contacts

8.1 I–V characteristics

Figure 13 shows the I–V characteristics of the fabricated ZnO MSM PDs (Pd/ZnO, Ni/ZnO and Pt/ZnO) on the PPC plastic measured without and with UV illumination (385 nm with power of 58.4 μW). Under dark environment, the current (I_d) at 0.8 volt was equal to 0.44, 1.72 and 1.90 □A and the ideality factor (n) was derived and found to be 1.37, 1.76 and 1.78 for PD with Pd, Ni and Pt contacts respectively..

On the other hand, when the sample was illuminated with UV wavelength of 385 nm with power of 58.4 μW; the photocurrent (I_{ph}) (at same voltage) biased at 0.8V was 5.27, 7.44 and 8.80 μA, and n was found to be 1.21, 1.46 and 1.50, respectively for the fabricated ZnO PD with Pd, Ni and Pt contact electrodes. Table 4 summarized the I-V characteristics with different values of I_d, I_{ph} and n for the PDs with Pd, Ni and Pt metal contacts.

Metal contact	Dark Environment			Illuminated Environment			Change of SBH (meV)
	Dark current, I_d (μA)	Ideality factor, n	SBH, ϕ_B (eV)	Photo current, I_{ph} (μA)	Ideality factor, n	SBH, ϕ_B (eV)	
Pd	0.44	1.37	0.738	5.27	1.21	0.700	38
Ni	1.72	1.76	0.705	7.44	1.46	0.672	33
Pt	1.90	1.78	0.700	8.80	1.50	0.668	32

Table 4. A summary of the I_d, I_{ph} and n for the PDs with Pd, Ni and Pt metal contacts

The results obtained for this study can be explained as follows: when light impinges onto the MSM UV detector, high-energy photons will be absorbed by the ZnO thin film, and with an appropriate bias, photon-generated carriers will drift toward the contact electrodes and a photocurrent will be observed (Young et al., 2006).

Further application of reverse bias acts to increase the electric field magnitude within the depletion region and to reduce the barrier height (Sze & Kwok 2006). When the energy of the incident photon is higher than the bandgap of ZnO, electron-hole pairs are generated inside ZnO thin film by light absorption. At the same time, the electron–hole pairs are separated by the electric field inside the depletion region of the ZnO thin film to generate the photocurrent.

In this study, the application of a bias on each of the Pd, Ni or Pt metallic fingers will create an electric field within the underlying ZnO thin film that sweeps the photo generated carriers out of the depletion region. The speed and the collection efficiency of the device vary, depending upon the magnitude of the applied bias, the finger separation and the average depth at which the photo generated carriers are produced (Jandow et al., 2010b).

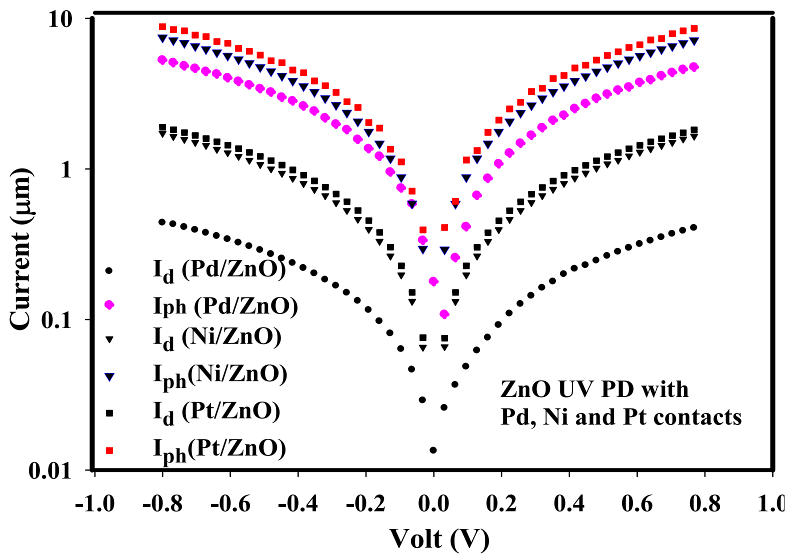

Fig. 13. Dark current (I_d) and photocurrent (I_{ph}) as a function of bias voltage (V) characteristics of the fabricated ZnO MSM PD with different electrodes type

Comparing among the three PDs, PD with Pd has the lowest dark current, this follows by Ni and Pt. the dark current for PT and Ni contacts are about 4.3 and 3.9 times of Pd. The difference of the dark current for PT and Ni contacts is relatively insignificant. This could be anticipated from the SBHs, as shown in Table 4. The difference of SBH value for these contacts is very small i.e. 5 meV.

8.2 Schottky barrier height calculation

As mentioned earlier, one of the most interesting properties of a metal-semiconductor (MS) interface is its Schottky barrier height (SBH), which is a measure of the mismatch of the energy levels for majority carriers across the MS interface. The SBH controls the electronic transport across MS interfaces and is, of vital importance to the successful operation of any semiconductor device (Tung et al., 2001). SBH plays an important role to modulate the dark and photo currents.

In particular, the forward-bias portion of the I-V characteristics has often been used to deduce the magnitude of SBH (Cho et al., 2000). The transport of carriers across a MS interface is very sensitively dependent on the magnitude of the energy barrier, SBH.

SBH for the three PDs could be determined by using Eqs. (3-8). Based on Eq. 8, the plot of $\ln\left\{I\exp\left(qV/\{KT\}\right)/\left[\exp\left(qV/\{KT\}\right)-1\right]\right\}$ vs. V for Pd contact is shown in Figure 14. I_0 was derived from the intercept with y-axis and by substituting this I_0 value in Eq. 4, ϕ_B was found to be 0.738 eV. Similarly for Ni/ZnO and Pd/ZnO, the ϕ_B determined from the plot under dark and illuminated conditions are summarized in Table 4.

Many metals such as Ag, Au, Pd and Pt have been used as Schottky contacts for ZnO, and resulted in SBH of between 0.6-0.8 eV (Gür et al., 2007).

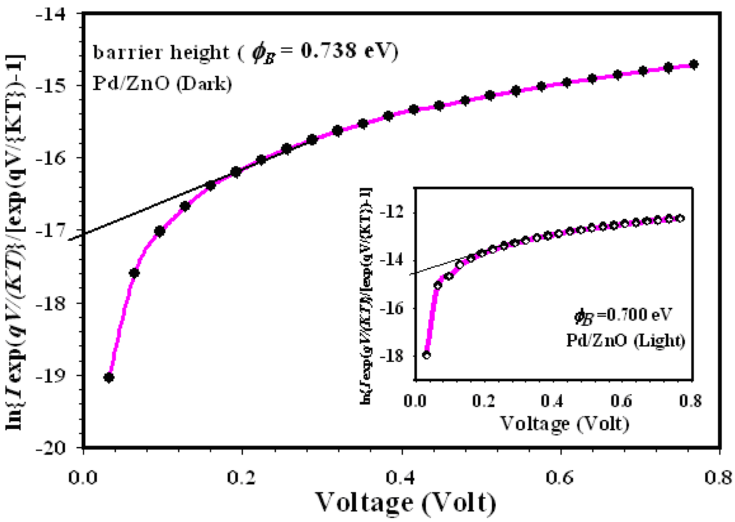

Fig. 14. $\ln\left\{I\exp\left(qV/\{kT\}\right)/\left[\exp\left(qV/\{kT\}\right)-1\right]\right\}$ vs V (under dark condition) of the fabricated ZnO MSM PD with Pd electrodes on PPC substrate. The inset shows ϕ_B calculation under illumination

From Figure 13 it can be found that the ZnO MSM UV PD with Pt electrode has the highest light current. That is because it has the lowest Schottky barrier height at the Pt/ZnO interface. While still the light current for the PD with Pd contact is the lowest for the same reason.

One can find that the difference among the electrical characteristics of the three PDs may mean that their barriers are different. Since the barrier height of the PD with Pd contact is higher than the barrier height for the PDs with Ni and Pt contacts, the integrated number of carriers above the barrier height for the PD with Pd contact will be less than the others, which caused the total current over the barrier to be lower. Eventually the lowest dark current was obtained with the Pd contact compares with the PDs with Ni and Pt contacts.

From Table 4, it was found that the calculated SBH value for the PD with Pd and Ni contacts is higher than that with Pt contact although the work function of Pt is the highest. This indicated that the barrier height is independent of the work function and many research groups (Kim et al., 2010; Wright et al., 2007; Ip et al., 2005; Liu et al 2004; Dong and Brillson, 2008; Kahng, 1063; Vanlaar and Scheer, 1965; Andrews and Phillips, 1975; Mead and Spitzer, 1963; Yıldırım et al., 2010; Roccaforte et al., 2010; Brillson et al., 2008; Rabadanov et al., 1982; Mead, 1966; Coppa et al., 2005) have reported that the barrier heights did not correlate with the metal work functions, suggesting many possible influences such as surface states, surface morphology, and surface contamination play important roles in the electrical properties of the contacts.

The increase of current when PD is illuminated by an UV source can be explained by work function of metal and semiconductor in the energy band diagram (Brillson et al., 2008; Rabadanov et al., 1982; Kim et al., 2010). In this case the metal and semiconductor are taken as Pd and ZnO.

ZnO which has a work function of ϕ_{ZnO}= 4.1 eV is also known to be a natural n-type semiconductor due to the oxygen vacancy which acts as trap center. The Pd work function (ϕ_{Pd} = 5.6 eV) is higher than that of ZnO. When a contact is formed electrons flow from ZnO to Pd metal until the Fermi levels align resulting in band bending as shown in Figure 15, where E_0, E_C, E_{FS}, E_V and □ are the vacuum level, the conduction band, the Fermi level, the valence band and the work function of the semiconductor (S) which in our case is ZnO, respectively, and E_{FM} is the Fermi level of the metal contact (M) which is Pd as shown in the figure, respectively. In ZnO, the trapping mechanism administrates the photoconduction. The oxygen molecules in the ZnO thin film surface capture electrons from the semiconductor. Under UV illumination, the photon energy releases the trapped electrons and also generates photo-induced electrons, causing an enhancement of the current.

The results obtained in this work are in agreement with the results reported by Young *et al* (Young et al., 2006) who fabricated ZnO MSM PD with Ag, Pd and Ni contact electrodes, and the barrier height for Ag/ZnO, Pd/ZnO and Ni/ZnO interfaces were 0.736, 0.701 and 0.613 eV, respectively although the work function for Ag =4.74, Pd =5.60 and Ni =5.42 eV. This result showed that although the work function of Ag is the lowest but the barrier height for Ag/ZnO was the highest, which indicated that the barrier height independent on the work function. Furthermore, Polyakov *et al* (Polyakov et al., 2003) results also showed that Schottky barrier heights were equal to 0.65-0.70 eV from capacitance-voltage measurements by using Au and Ag Schottky contacts on the bulk n-ZnO crystals; Au/ZnO SBH was lower than Ag/ZnO even though the work function of Au 5.47 is higher than the Ag. As well as, Neville and Mead (Neville & Mead 1970) results showed the barrier energy for Au is 0.66 eV and for Pd is 0.60 eV dependent on the forward current-voltage characteristics and as mentioned earlier the work function of Pd is higher than Au.

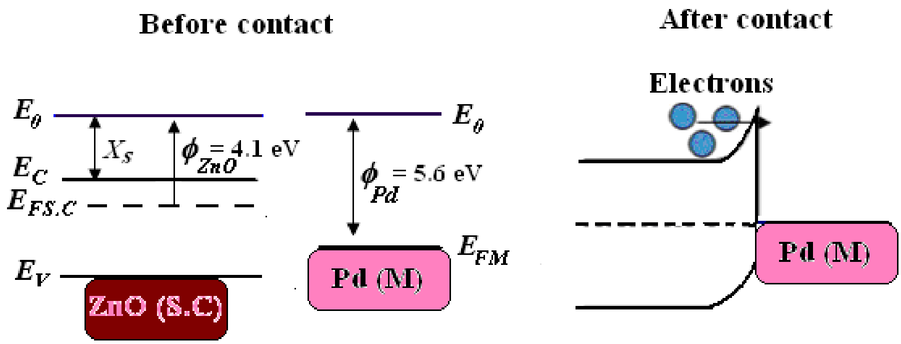

Fig. 15. The energy band diagram of ZnO and Pd.

The independence of SBH on the metal work function has been explained by many researchers (Brillson et al., 2008; Rabadanov et al., 1981; Mead, 1966; Coppa et al., 2005), they pointed out SBH could be affected by the interface structure and the associated interface states

8.3 Responsivity and quantum efficiency

Figure 16 shows the responsivity as a function of the incident wavelength for the three ZnO MSM UV PDs with Pd, Ni and Pt contact electrodes. At 0.8 V and by applying Eq. 9, it was found that the maximum responsivity for the three PDs were found to be 0.08, 0.09 and 0.11 A/W, which corresponds to quantum efficiency (η %) of 27.1 % 31.7 % and 37.7% respectively which are shown in Figure 17. It is observed that the PD with Pt contacts has higher responsivity and quantum efficiency comparing to the PDs with Pd and Ni contacts due to the lowest barrier height and highest photocurrent. Table 5 summarizes the responsivity and quantum efficiency for Pd, Ni and Pt contacts, respectively.

As shown in the figure, the PD responsivity was nearly constant in the UV region ~ 320–360 nm; it started to increase from 365 nm, of which the responsivity peaked at 385 nm and began to decrease whenever became close to the visible region. This can be explained as follows; when ZnO detector is irradiated by UV light with energy higher than the bandgap (3.37 eV for ZnO), electron–hole pairs will be generated, as a result these excess charge carriers contribute to photo current and result in the response to the UV light. The cut-off at wavelength of 385 nm is nearly close to the ZnO energy bandgap of 3.37 eV; the responsivity decreased at the shorter wavelength range due to the decrease of the penetrating depth of the light, resulting in an increase of the surface recombination (Young et al 2007; Jandow et al., 2010a; Yan et al., 2004).

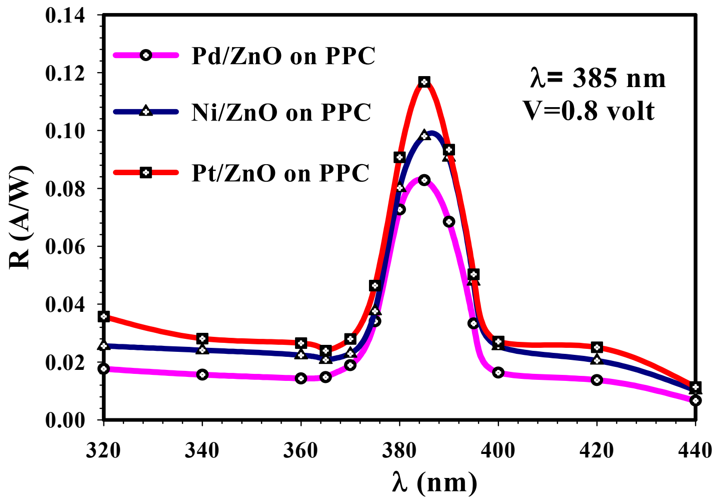

Fig. 16. Measured spectral responsivity of the three fabricated ZnO MSM PDs with different electrodes on PPC substrate

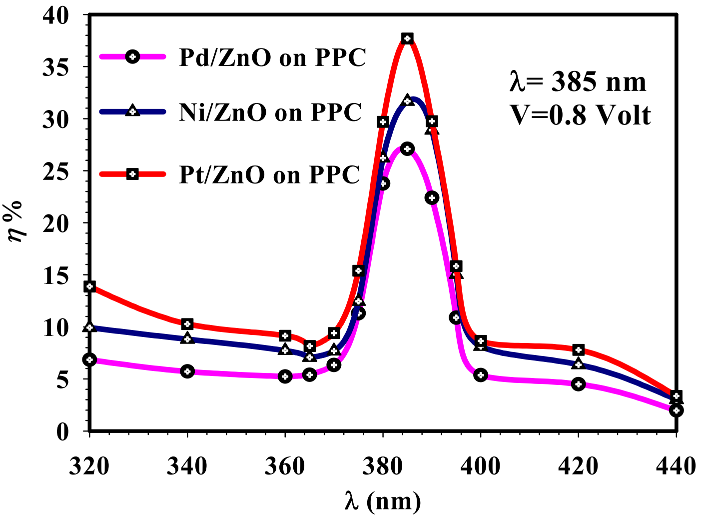

Fig. 17. Quantum efficiency of the three fabricated ZnO MSM PDs with different electrodes on PPC substrate

Metal contacts	Responsivity (R) (A/W)	Quantum efficiency (η %)
Pd	0.082	27.1
Ni	0.098	31.7
Pt	0.116	37.7

Table 5. A summary of the responsivity (R) and quantum efficiency (η %) values for the PDs with Pd, Ni and Pt metal contacts at 0.8 volt

9. Conclusion

In summary, an overview of the characteristics of the deposited ZnO thin film on various organic substrates such as polyethylene terephthalate (PET), polyolefin, polytetrafluoroethylene (Teflon) and Polycarbonate (PC) and their potential applications in various areas has been presented. A review of semiconductor PDs, types of PDs as well as their characteristics has been demonstrated. Apart from that, the properties of the ZnO thin films deposited on PPC plastic substrate have been expressed. ZnO UV detectors prepared on PPC substrate with different electrodes i.e. Pd, Ni and Pt have been fabricated and investigated. The results showed that the deposited ZnO thin film had good structural and optical properties. In addition ZnO UV PDs fabricated on PPC with different metal contacts showed that Pt/ZnO MSM UV PD has the highest quantum efficiency.

10. Acknowledgments

This work was conducted under the grant no. (100/PFIZIK/8/4010) support from Universiti Sains Malaysia is gratefully acknowledged.

11. References

Andrews. J. & Phillips, J. (1975). Chemical bonding and structure of meta semiconductor interfaces. *Phys. Rev. Lett.*, Vol.35, No.1, pp. 56-59

Angelats, L. (2006). "Silva Study of structural, electrical, optical and magnetic properties of ZnO based films produced by magnetron sputtering" PhD thesis, university of Puerto Rico UPR

Auret, F., Meyer, W., Rensburg, P., Hayes, M., Nel, J., Wenckstern, H., Schmidt, H., Biehne, G., Hochmuth, H., Lorenz, M., Grundmann, M. (2007). Electronic properties of defects in pulsed-laser deposition grown ZnO with levels at 300 and 370meV below the conduction band. *Physica B*, Vol.401-402, pp. 378-381

Banerjee, A., Ghosh, C., Chattopadhyay, K., Minoura, H., Sarkar, A., Akiba, A., Kamiya, A., & Endo, T. (2006). Low-temperature deposition of ZnO thin films on PET and glass substrates by DC-sputtering technique. *Thin Solid Films*, Vol.496, pp. 112-116

Banerjee, A., Ghosh, C., Chattopadhyay, K., Minoura, H., Sarkar, A., Akiba, A., Kamiya, A., & Endo, T. (2006). Low-temperature deposition of ZnO thin films on PET and glass substrates by DC-sputtering technique. *Thin Solid Films*, Vol.496, pp. 112-116

Bang, K.-H., Hwang, D.-K., & Myoung, J.-M. (2003). Effects of ZnO buffer layer thickness on properties of ZnO thin films deposited by radio-frequency magnetron sputtering. *Appl. Surf. Sci.*, Vol.207, pp. 359-364

Basak, D., Amin, G., Mallik, B., Paul, G., & Sen, S. (2003). Photoconductive UV detectors on sol-gel-synthesized ZnO films. *J. Cryst. Growth*, Vol.256, pp. 73-77

Brabec, C., Sariciftci, N., & Hummelen, J. (2001). Plastic Solar Cells. *Adv. Funct. Mater.*, Vol.11, No.1, pp. 15-26

Brillson, L., Mosbacker, H., Hetzer, M., Strzhemechny, Y., Look, D., Cantwell, G., Zhang, J., & Song, J. (2008). Surface and near-surface passivation, chemical reaction, and Schottky barrier formation at ZnO surfaces and interfaces. *Appl. Surf. Sci.,* Vol.254, pp. 8000-8004

Brillson, L., Mosbacker, H., Hetzer, M., Strzhemechny, Y., Look, D., Cantwell, G., Zhang, J., & Song, J. (2008). Surface and near-surface passivation, chemical reaction, and Schottky barrier formation at ZnO surfaces and interfaces. *Appl. Surf. Sci.,* Vol.254, pp. 8000–8004

Caria, M., Barberini, L., Cadeddu, S., Giannattasio, A., Lai, A., Rusani, A., & Sesselego, A. (2001). Far UV responsivity of commercial silicon photodetectors. *Nucl. Instrum. Meth. A*, Vol.466, No.1, pp. 115-118

Chakraborty, A., Mondal, T., Bera, S., Sen, S., Ghosh, R., & Paul, G. (2008). Effects of Aluminium and Indium incorporation on the structural and optical properties of ZnO thin films synthesized by spray pyrolysis. *Mater. Chem. Phys*., Vol.112, pp. 162-166

Chang, S., Chang, S., Chiou, Y., Lu, C., Lin, T., Lin, Y., Kuo, C., & Chang, H. (2007). ZnO photoconductive sensors epitaxially grown on sapphire substrates. *Sensor. Actuator., A*, Vol.140, pp. 60-64

Cho, H., Leerungnawarat, P., Hays, D., Pearton, S., Chu, S., Strong, R., Zetterling, C.-M., Östling, M., & Ren, F. (2000). low-damage dry etching of SiC. *Appl. Phys. Lett*., Vol.76, No.6, pp. 739-741

Coppa, B., Fulton, C., Kiesel, S., Davis, R., Pandarinath, C., Burnette, J., Nemanich, R., & Smith, D. (2005). Structural, microstructural, and electrical properties of gold films and Schottky contacts on remote plasma-cleaned, n-type ZnO{0001} surfaces. *J. Appl. Phys*., Vol.97. pp. 103517-1-13

Coppa, B., Fulton, C., Kiesel, S., Davis, R., Pandarinath, C., Burnette, J., Nemanich, R., & Smith, D. J. (2005). Structural, microstructural, and electrical properties of gold films and Schottky contacts on remote plasma-cleaned, n-type ZnO{0001} surfaces. *J. Appl. Phys*. Vol.97, pp. 103517-1-13

Craciun, V., Elders J., Gardeniers, J., & Boyd, I. (1994). Characteristics of high quality ZnO thin films deposited by pulsed laser deposition. *Appl. Phys. Lett*., Vol. 65, No.23, pp. 2963-2965

Daraee, M., Hajian, M., Rastgoo, M., & Lavasanpour, L. (2008). Study of electrical characteristic of surface barrier detector with high series resistance. *Adv. Studies Theor. Phys*., Vol.2, No.20, pp. 957-964.

Dong, Y. & Brillson, L. (2008). First-principles studies of metal (111)/ZnO {0001} interfaces. *J. Eectron. Mater*., Vol.37, No.5, pp. 743-748

Ergin, B., Ketenci, E., & Atay, F. (2009). Characterization of ZnO films obtained by ultrasonic spray pyrolysis technique. *Int. J. Hydrogen Energ*., Vol.34, pp. 5249-5254

Gao, W., & Li, Z. (2004). ZnO thin films produced by magnetron sputtering. *Ceram. Int.,* Vol.30, pp. 1155-1159

Ghosh, R., Basak, D., & Fujihara, S. (2004). Effect of substrate-induced strain on the structural, electrical, and optical properties of polycrystalline ZnO thin films. *J. Appl. Phys*., Vol.96, No.5, pp. 2689-2692

Gökkavas, M., Butun, S., Tut, T., Biyikli, N., & Ozbay, E. (2007). AlGaN-based high-performance metal–semiconductor–metal photodetectors. *PNFA*., Vol.5, pp. 53-62

Gümüş, C., Ozkendir, O., Kavak, H., & Ufuktepe, Y. (2006). Structural and optical properties of zinc oxide thin films prepared by spray pyrolysis method. *J. Optoelectron. Adv. M*., Vol.8, No.1, pp. 299-303

Gür, E., Tüzemen, S, Kılıç, B., & Coşkun, C. (2007). High-temperature Schottky diode characteristics of bulk ZnO. *J. Phys.: Condens. Matter*., Vol.19, pp. 196206-196214

Haas, F. (1997). Principles of Semiconductor Devices. RL-TR-96-217, In-House Report

Hanzaz, M., Bouhdada, A., Vigué, F., & Faurie, J. (2007). ZnSe-and GaN-based Schottky barrier photodetectors for blue and ultraviolet detection. *J. Act. Pass. Electron. Dev.*, Vol.2, pp. 165-169

Hickernell, F. (1976). Zinc-Oxide Thin-film surface-wave transducers. *Proceedings of the IEEE*, Vol. 64, No.5, pp. 631-635

Hiramatsu, K., & Motogaito, A. (2003). GaN-based Schottky barrier photodetectors from near ultraviolet to vacuum ultraviolet (360-50 nm). *phys. stat. sol. (a)*, Vol.195, No.3, pp. 496-501

Hussain, S. (2008). "Investigation of Structural and Optional Properties of Nanpcrystalline ZnO" PhD thesis, Department of Physics, Chemistry and Biology Linköping University

Hwang, K-S. , Kang, B-A., Jeong, J-H. , Jeon Y-S. , & Kim B-H. (2007). Spin coating-pyrolysis derived highly c-axis-oriented ZnO layers pre-fired at various temperatures. *Curr. Appl. Phys*., Vol.7, pp. 421-425

Ianno, N., McConville, L., Shaikh, N., Pittal, S., & Snyder, P. (1992). Characterization of pulsed laser deposited Zinc oxide. *Thin Solid Films*, Vol.220, pp. 92- 99

Ip, K., Khanna, R., Norton, D., Pearton, S., Ren, F., Kravchenko, I., Kao, C., & Chi, G. (2005). Thermal stability of W2B and W2B5 contacts on ZnO. *Appl. Surf. Sci*., Vol.252, pp. 1846-1853

Jandow N. N., F. K. Yam, S. M. Thahab, H. Abu Hassan, & Ibrahim, K. (2010a). Characteristics of ZnO MSM UV photodetector with Ni contact electrodes on Poly Propylene Carbonate (PPC) plastic substrate. *Curr. Appl. Phys*., Vol.10, pp. 1452-1455

Jandow, N., Ibrahim, K., Abu Hassan, H. (2010b). I-V Characteristic for ZnO MSM Photodetector with Pd Contact Electrodes on PPC Plastic, *AIP Conf. Proc*., Vol.1250, pp. 424-427

Jandow, N., Ibrahim, K., Abu Hassan, H., Thahab, S., & Hamad, O. (2010c). The electrical properties of ZnO MSM Photodetector with Pt Contact Electrodes on PPC Plastic. *JED*, Vol.7, pp. 225-229

Jandow, N., Ibrahima, K., Yam, F., Abu Hassan, H., Thahab, S., & Hamad, O. (2010d). The study of ZnO MSM UV photodetector with Pd contact electrodes on (PPC) plastic. *J.Optoelectron. Adv. Mat.-Rabid*, Vol.4, No.5, pp. 726-730

Jandow, N., Yam, F., Thahab, S., Ibrahim, K., Abu Hassan, H. (2010). The characteristics of ZnO deposited on PPC plastic substrate. *Mater. Lett*., Vol.64, pp. 2366-2368

Janotti, A., & Van de Walle, C. (2009e). Fundamentals of zinc oxide as a semiconductor. *Rep. Prog*. Phys., Vol. 72, pp. 126501-126530

Jeong, I.-S., Kim, J., Park, H.-Ho, & Im, S. (2004). n-ZnO/p-Si UV photodetectors employing AlO_x films for antireflection. *Thin Solid Films*, Vol.447-448, pp. 111-114

Jiang, D., Zhang, J., Lu, Y., Liu, K., Zhao, D., Zhang, Z., Shen, D., & Fan, X. (2008) Ultraviolet Schottky detector based on epitaxial ZnO thin film. *Solid State Electron*., Vol.52, pp. 679-682

Jin, B., Woo, H., Im, S., Bae, S., & Lee, S. (2001). Relationship between photoluminescence and electrical properties of ZnO thin films grown by pulsed laser deposition. *Appl. Surf. Sci.*, Vol.169-170, pp. 521-524

Jin, C. (2003). "Growth and characterization of ZnO and ZnO-based Alloys-MgxZn1-xO and MnxZn1-xO". PhD thesis, Department of materials science and Engineering, North Carolina state university, Raleigh

Jun, W., Degang, Z., Zongshun, L., Gan F., Jianjun, Z., Xiaomin, S., Baoshun, Z., & Hui, Y. (2003). Metal-semiconductor-metal ultraviolet photodetector based on GaN. *Sci. China Ser. G*, Vol.46, No.2, pp. 198-203

Kahng, D. (1963). Conduction properties of the Au-n-type-Si Schottky barrier. *Solid State Electron.*, Vol. 6, pp. 281-295

Kang, S., Joung, Y., Chang, D., & Kim, K. (2007). Piezoelectric and optical properties of ZnO thin films deposited using various $O_2/(Ar+O_2)$ gas ratios. *J. Mater. Sci: Mater Electron.*, Vol.18, pp. 647-653

Khoury, A., al Asmar, R., Abdallah, M., El Hajj Moussa, G., & Foucaran, A. (2010). Comparative study between zinc oxide elaborated by spray pyrolysis, electron beam evaporation and rf magnetron techniques. *Phys. Status Solidi A*, Vol.207, No.8, pp. 1900-1904

Kim, H., Kim, H., & Kim, D.-W. (2010). Silver Schottky contacts to a-plane bulk ZnO. *J. Appl. Phy.*, Vol.108, pp. 074514-1-5

Kim, J., Lee J., Lee, J., Lee, D., Jang, B., Kim, H., Lee W., Cho, C., & Kim, J. (2009). Characteristics of ZnO films deposited on plastic substrates at various rf sputtering powers. *J. Korean Phys. Soc.*, Vol.55, No.5, pp. 1910-1914

Kim, J., Yun, J., Kim, C., Park, Y., Woo, J., Park, J., Lee, J., Yi, J., & Han, C. (2010). ZnO nanowire-embedded Schottky diode for effective UV detection by the barrier reduction effect. *Nanotechnology*, Vol.21, pp. 115205-115210

Kiriakidis, G., Suchea, M., Christoulakis, S., Horvath, P., Kitsopoulos, T., & Stoemenos, J. (2007). Structural characterization of ZnO thin films deposited by dc magnetron sputtering. *Thin Solid Films*, Vol.515, pp. 8577-8581

Koch, U., Fojtik, A., Weller, H., & Henglein, A. (1985). Photochemistry of semiconductor colloids, preparation of extremely small ZnO particles, fluorescence phenomena and size quantization effects, *Chem.Phys.Lett.,* Vol.122, pp. 507-510

Kumar, S., Kim, H.., Sreenivas, K., & Tandon, P. (2009). ZnO based surface acoustic wave ultraviolet photo sensor. *J. Electroceram*, Vol.22, pp. 198-202

Lai, L.-W., & Lee, C.-T. (2008). Investigation of optical and electrical properties of ZnO thin films, *Mater. Chem. Phys.*, Vol.110, pp. 393-396

Lakhotia, G., Umarji, G., Jagtap, S., Rane, S., Mulik, U., Amalnerkar, D., & Gosavi, S. (2010). An investigation on TiO_2-ZnO based thick film 'solar blind', photo-conductor for 'green' electronics. *Mater. Sci. Eng. B*, Vol.168, pp. 66-70

Liang, S., Sheng, H., Liu, Y., Huo, Z., Lu, Y., & Shen, H. (2001). ZnO Schottky ultraviolet photodetectors. *J. Cryst. Growth*, Vol.225, pp. 110-113

Lim, J., Kang/ Ch., Kim, K., Park, I., Hwang, D., & Park, S. (2006). UV Electroluminescence Emission from ZnO light-emitting diodes grown by high-temperature radiofrequency sputtering. *Adv. Mater.*, Vol.18, pp. 2720-2724

Lin, T., Chang, S., Su, Y., Huang, B., Fujita, M., & Horikoshi, Y. (2005). ZnO MSM photodetectors with Ru contact electrodes. *J. Cryst. Growth*, Vol.281, pp. 513-517

Liu, K., Ma, J., Zhang, J., Lu, Y., Jiang, D., Li, B., Zhao, D., Zhang, Z., Yao, B., & Shen, D. (2007). Ultraviolet photoconductive detector with high visible rejection and fast photoresponse based on ZnO thin film. *Solid State Electron.*, Vol.51, pp. 757-761

Liu, K., Sakurai, M., & Aono, M. (2010). ZnO-based ultraviolet photodetectors. *Sensors*, Vol.10, pp. 8605-8630

Liu, Y., Egawa, T., Jiang, H., Zhang, B., Ishikawa, H., & Hao, M. (2004). Near-ideal Schottky contact on quaternary AlInGaN epilayer lattice-matched with GaN, *Appl. Phys. Lett.*, Vol.85, No.24, pp. 6030-6032

Liu, Y., Gopla, C., Liang, S., Emanetoglu, N., Lu, Y., Shen, H., & Wraback, M. (2000). Ultraviolet detectors based on epitaxial ZnO films grown by MOCVD. *J. Electron. Mater*, Vol.29, No.1, pp. 69-74

Liu, Y., Li, Q., & Shao, H. (2009). Properties of ZnO-Al films deposited on polycarbonate substrate. *Vacuum*, Vol.83, pp. 1435–1437

Liu, Y.-Y., Yuan, Y. –Z., Gao, X.-T., Yan, S.-S., Cao, X.-Z., & Wei, G.-X. (2007). Deposition of ZnO thin film on polytetrafluoroethylene substrate by the magnetron sputtering method. *Mater. Lett.,* Vol.61, pp. 4463-4465

Lu, X., Zhu, Q., & Meng, Y. (2005). Kinetic analysis of thermal decomposition of Poly(Propylene Carbonate), *Polym. Degrad. Stab.*, Vol.89, pp. 282-288

Lu, Y.-M., Tsai, S.-Y., Lu, J.-J., & Hon, M.-H. (2007). The structural and optical properties of zinc oxide thin films deposited on PET substrate by rf. magnetron sputtering. *Solid State Phenom.*, Vol.121-123, pp. 971-974

Ma, C., Taya, M., & Xu, C. (2008). Flexible electrochromic device based on poly (3, 4-(2, 2-dimethylpropylenedioxy) thiophene). *Electrochim. Acta*, Vol.54, pp. 598-605

Mahmood, F., Gould, R., Hassan, A., & Salih, H. (1995). DC. properties of ZnO thin films prepared by rf. magnetron sputtering. *Thin Solid Films*, Vol.770, pp. 376-379

Mandalapu, L., Xiu, F., Yang, Z., & Liu, J. (2007). Ultraviolet photoconductive detectors based on Ga-doped ZnO films grown by molecular-beam epitaxy. *Solid State Electron.*, Vol.51, pp. 1014-1017

Mead, C. (1966). Metal-semiconductor surface barriers. *Solid State Electron.*, Vol.9, pp. 1023-1033

Mead, C., & Spitzer, W. (1963). Fermi level position at semiconductor surfaces. *Phys. Rev. Lett.*, Vol.10, No.11, pp. 471-472

Monroy, E., Omnés, F., & Calle, F. (2003). Wide-bandgap semiconductor ultraviolet photodetectors. *Semicond. Sci. Technol.*, Vol.18, pp. R33-R51

Moon, T.-H., Jeong, M.-C., Lee, W., & Myoung, J.-M. (2005). The fabrication and characterization of ZnO UV detector. *Appl. Surf. Sci.*, Vol.240, pp. 280-285

Myoung, J.-M., Yoon, W.-H., Lee, D.-H., Yun, I., Bae, S.-H., & Lee, S.-Y. (2002). Effects of thickness variation on properties of ZnO thin films grown by pulsed laser deposition, *Jpn. J. Appl. Phys.*, Vol.41, pp. 28-31

Nandy, S., Goswami, S., & Chattopadhyay, K. (2010). Ultra smooth NiO thin films on flexible plastic (PET) substrate at room temperature by rf magnetron sputtering and effect of oxygen partial pressure on their properties, *Appl. Surf. Sci.*, Vol.256, pp. 3142-3147

Nause, J., & Nemeth, B. (2005). Pressurized melt growth of ZnO boules. *Semicond. Sci. Technol.*, Vol.20, pp. S45-S48

Nav Bharat Metallic Oxide Industries Pvt. Limited. n.d. *Some of the popular applications of Zinc Oxide*. Available from: <http://www.navbharat.co.in/Clients.htm>

Neville, R., & Mead, C. (1970). "Surface barriers on zinc oxide". *J. Appl. Phys.*, Vol.41, No.9, pp. 3795- 3800

Nunes, P., Fortunato, E., & Martins, R. (2001). Influence of the annealing conditions on the properties of ZnO thin films. *Int. J. Inorg. Mater.*, Vol.3, pp. 1125-1128

Ott, A., & Chang, R. (1999). Atomic layer-controlled growth of transparent conducting ZnO on plastic substrates. *Mater. Chem. Phys.*, Vol.58, pp. 132-138

Paul, G., Bhaumik, A., Patra, A., & Bera, S. (2007). Enhanced photo-electric response of ZnO/polyaniline layer-by-layer self-assembled films, *Mater. Chem. Phys.*, Vol.106, pp. 360-363

Plaza, J., Martínez, O., Carcelén, V., Olvera, J., Sanz, L., & Diéguez, E. (2008). Formation of ZnO and Zn1-xCdxO films on CdTe/CdZnTe single crystals. *Appl. Surf. Sci.*, Vol.254, pp. 5403-5407

Polyakov, A., Smirnov, N., Kozhukhova, E., Vdovin, V., Ip, K., Heo, Y., Norton, D., & Pearton, S. (2003). "Electrical characteristics of Au and Ag Schottky contacts on n-ZnO". *Appl. Phys. Lett.*, Vol.83, No.8, pp. 1575-1577

Rabadanov, R., Guseikhanov, M., Aliev, I., & Semiletov, S. (1981). Properties of metal-zinc oxide contacts. *Russ. Phys. J.*, Vol.24, No.6, pp. 548-551

Rabadanov, R., Guseikhanov, M., Aliev, I., & Semiletov, S. (1982). Properties of metal-zinc oxide contacts. *Russ Phys J.*, Vol.24, No.6, pp. 548-551

Rao, T., Kumar, M., Safarulla, A., Ganesan, V., Barman, S., & Sanjeeviraja, C. (2010). Physical properties of ZnO thin films deposited at various substrate temperatures using spray pyrolysis. *Physica B*, Vol.405, pp. 2226-2231

Roccaforte, F., Giannazzo, F., Iucolano, F., Eriksson, J., Weng, M., & Raineri, V. (2010). Surface and interface issues in wide band gap semiconductor electronics. *Appl. Surf. Sci.*, Vol.256, pp. 5727-5735

Sans, J., Segura, A., Mollar, M., & Marí, B. (2004). Optical properties of thin films of ZnO prepared by pulsed laser deposition. *Thin Solid Films*, Vol.453-454, pp. 251-255

Shan, F., Liu, G., Lee, W., Lee, G., Kim, I., Shin, B., & Kim, Y. (2005). Transparent conductive ZnO thin films on glass substrates deposited by pulsed laser deposition. *J. Cryst. Growth*, Vol.277, pp. 284-292

Shan, F., Shin, B., Jang, S., & Yu, Y. (2004). Substrate effects of ZnO thin films prepared by PLD technique. *J. Eur. Ceram. Soc.*, Vol.24, pp. 1015-1018

Sofiani, Z., Derkowska, B., Dalasińsk, P., Wojdyła, M., Dabos-Seignon, S., Alaoui Lamrani, M., Dghoughi, L., Bała, W., Addou, M., Sahraoui, B. (2006). Optical properties of ZnO and ZnO:Ce layers grown by spray pyrolysis. *Opt. Commun.*, Vol.267, pp. 433-439

Song, P.-f., Wang, S.-j., Xiao, M., Du, F.-g., Gan, L.-q., Liu, G.-q., & Meng, Y.-z. (2009). Cross-linkable and thermally stable aliphatic polycarbonates derived from Co_2, propylene oxide and maleic anhydride. *J Polym Res*, Vol.16, pp. 91-97

Sze, S. (2002). Semiconductor devices, physics and technology, 2nd ed., John Wiley & Sons New York , USA

Sze, S., & Kwok K. (2006). Physics of semiconductor devices, 3rd ed., United States of America

Sze, S., Coleman, D., & Loya, J., (1971). Current transport in metal-semiconductor-metal (MSM) structures. *Solid State Electron*., Vol.14, pp. 1209-1218

Tan, S., Chen, B., Sun, X., Fan, W., Kwok, H., Zhang, X., & Chua, S. (2005). Blueshift of optical band gap in ZnO thin films grown by metal-organic chemical-vapor deposition. *J. Appl. Phys*., Vol.98, pp. 013505-013505-5

Tneh, S., Hassan, Z., Saw, K., Yam, F., Abu Hassan, H. (2010). The structural and optical characterizations of ZnO synthesized using the ''bottom-up'' growth method. *Physica B*, Vol.405, pp. 2045-2048

Tsai, H-Y. (2007). Characteristics of ZnO thin film deposited by ion beam sputter. *J. Materi. Process. Technol*., Vol.192-193, pp. 55-59

Tsai, S.-Y., Lu, Y.-M., Lu, J.-J., & Hon, M.-H. (2006). Comparison with electrical and optical properties of zinc oxide films deposited on the glass and PET substrates. *Surf. Coat. Technol*., Vol.200, pp. 3241-3244

Tung, R. (2001). Recent advances in Schottky barrier concepts. *Mater. Sci. Eng*., *R,* Vol.35, pp. 1-138

Tüzemen, S., & Gür, E. (2007). Principal issues in producing new ultraviolet light emitters based on transparent semiconductor zinc oxide. *Opt. Mater*., Vol.30, pp. 292-310

Vanlaar, J. & Scheer, J. (1965). Fermi level stabilization at semiconductor surfaces. *Surf. Sci*. Vol.3, pp. 189-201

Wang, Q., Pflügl, C., Andress, W., Ham, D., & Capasso, F. (2008). Gigahertz surface acoustic wave generation on ZnO thin films deposited by radio frequency magnetron sputtering on III-V semiconductor substrates. *J. Vac. Sci. Technol. B*, Vol.26, No.6, pp. 1848-1851

Wei, X., Zhang, Z., Liu, M., Chen, C., Sun, G., Xue, C., Zhuang, H., & Man, B. (2007) Annealing effect on the microstructure and photoluminescence of ZnO thin films. *Mater. Chem. Phys*., Vol.101, pp. 285-290

Wright, J., Stafford, L., Gila, B., Norton, D., Pearton, S., Wang, H.-T., & Ren, F. (2007). Effect of cryogenic temperature deposition of various metal contacts on bulk single-crystal n-type ZnO, *J. Electron. Mater*., Vol.36, No.4, pp. 488-493

Wu, L., Tok, A., Boey, F., Zeng, X., & Zhang, X. (2007). Chemical Synthesis of ZnO Nanocrystals. *IEEE. Trans. Nanotechnol*, Vol.6, No.5, pp. 497-503

Yam, F., & Hassan, Z. (2008). The investigation of dark current reduction in MSM photodetector based on porous GaN. *J. Optoelectron Adv. M*., Vol.10, pp. 545-548

Yan, F., Xin, X., Aslam, S., Zhao, Y., Franz, D., Zhao, J., & Weiner, M. (2004). 4H-SiC UV Photo detectors with large area and very high specific detectivity. *IEEE J. Quantum Elect*., Vol.40, No.9, pp. 1315-1320

Yıldırım, N., Ejderha, K., & Turut, A. (2010). On temperature-dependent experimental I-V and C-V data of Ni/n-GaN Schottky contacts. *J. Appl. Phys*., Vol.108, pp. 114506-1-8

Young, S., Ji, L., Chang, S., & Su, Y. (2006). ZnO metal–semiconductor–metal ultraviolet sensors with various contact electrodes. *J. Cryst. Growth*, Vol.293, pp. 43-47.

Young, S., Ji, L., Chang, S., Chen, Y., Lam, K., Liang, S., Du, X., Xue, Q., & Sun, Y. (2007). ZnO metal-semiconductor-metal ultraviolet photodetectors with Iridium contact electrodes. *IET Optoelectron*., Vol.1, No.3, pp. 135-139

Young, S., Ji, L., Fang, T., Chang, S., Su, Y., & Du X. (2007). ZnO ultraviolet photodiodes with Pd contact electrodes. *Acta Mater*., Vol.55, pp. 329-333

Zhang, B., Wakatsuki, K., Binh, N., Usami, N., & Segawa, Y. (2004). Effects of growth temperature on the characteristics of ZnO epitaxial films deposited by metalorganic chemical vapor deposition. *Thin Solid Films*, Vol.449, pp. 12-19

Zhang, J., Kang, J., Hu, P., & Meng, Q. (2007). Surface modification of poly(propylene carbonate) by oxygen ion implantation. *Appl. Surf. Sci*., Vol.253, pp. 5436-5441

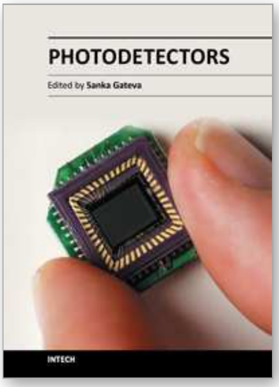

Photodetectors

Edited by Dr. Sanka Gateva

ISBN 978-953-51-0358-5
Hard cover, 460 pages
Publisher InTech
Published online 23, March, 2012
Published in print edition March, 2012

In this book some recent advances in development of photodetectors and photodetection systems for specific applications are included. In the first section of the book nine different types of photodetectors and their characteristics are presented. Next, some theoretical aspects and simulations are discussed. The last eight chapters are devoted to the development of photodetection systems for imaging, particle size analysis, transfers of time, measurement of vibrations, magnetic field, polarization of light, and particle energy. The book is addressed to students, engineers, and researchers working in the field of photonics and advanced technologies.